



Contents lists available at [www.sciencedirect.com](http://www.sciencedirect.com)

# Journal of the European Ceramic Society

journal homepage: [www.elsevier.com/locate/jeurceramsoc](http://www.elsevier.com/locate/jeurceramsoc)



## Tape casting and characterization of $\text{Li}_{2.08}\text{TiO}_3\text{-LiF}$ glass free LTCC for microwave applications

J.J. Bian\*, Q. Yu, J.J. He

Department of Inorganic materials, Shanghai University 333 NanChen Road, Shanghai, 200444, China

### ARTICLE INFO

#### Article history:

Received 2 September 2016

Received in revised form

20 September 2016

Accepted 22 September 2016

Available online xxx

#### Keywords:

Tape casing

Glass-free LTCC

Microwave dielectric properties

Sintering kinetics

### ABSTRACT

$\text{Li}_{2.08}\text{TiO}_3\text{-LiF}$  Glass-free Low temperature co-fired ceramic (LTCC) green tapes were prepared by tape casing technique. The rheology of the slurry was characterized using rheometer. The slurry exhibited pseudoplastic behavior. The sintering kinetics of the green tape was investigated using heating microscope. The sintering activation energy was determined to be  $\sim 173 \text{ kJ/mol}$ . The green tape could be densified at  $900^\circ\text{C}/2 \text{ h}$ . Microwave dielectric properties of the sintered tape were characterized in a split-post dielectric resonator using a network analyzer. The ceramic sheet with thickness of 0.11 mm demonstrated good microwave dielectric properties:  $\epsilon_r = 22.4$  and  $Q \times f = 35,490 \text{ GHz}$ . The cross sectional microstructure of the cofired multilayer stack was observed by scanning electron microscopy (SEM). The green tape demonstrated good chemical and shrinkage compatibilities with Ag electrode during sintering process. The thermal expansion coefficient and thermal conductivity of the ceramic is  $22.4 \text{ ppm}/^\circ\text{C}$  and  $4.75 \text{ W m}^{-1} \text{ K}^{-1}$ , respectively.

© 2016 Published by Elsevier Ltd.

### 1. Introduction

Low temperature co-fired ceramic (LTCC) technology has large benefits in microwave applications including miniaturization, multi-functionality, lighter weight, lower cost and higher performance of the devices. High conductive metal such as Ag is used as internal electrode in general. It requires that the sintering temperature of the ceramic should be less than  $950^\circ\text{C}$  so as to be co-fired with Ag electrode. Chemical and shrinkage compatibilities with silver electrode up to sintering temperature are indispensable [1]. In addition, good microwave dielectric properties including suitable relative dielectric permittivity, low dielectric loss and temperature stable of dielectric properties for the ceramic are also strongly required. High thermal conductivity is also desirable to conduct and dissipate the excess heat generated in multifunctional modules [2]. The metallization pastes will be screen printed layer by layer upon the green ceramic tape followed by stacking and lamination under pressure. The multilayer stack will be sintered below the melting point of the metal. Therefore, the development of flexible green tapes is one of the critical technological issues in practical LTCC applications.

Tape casting is a suitable forming technique to produce the thin flat green ceramic tape with large area and widely used in the production of ceramic substrate and multilayer component. Preparation of homogeneous ceramic slurry with good flowing properties is a key step for tape casting process. The slurry for tape casting should have good dispersion stability, suitable viscosity, pseudoplastic (shear-thinning) rheology property and high solid loading [3]. In a typical non-aqueous tape casting ceramic slurry the organic components usually consist of solvent, dispersant, binder and plasticizer. Preparing a dense, homogeneous green ceramic tape is a prerequisite to achieve dense, homogeneous, sintered ceramic sheet. High solid loading slurry is helpful to obtain a dense green tape with well packed microstructure [3]. However, achieving a high solid loading for tape casting slurry is not straightforward. The higher the solid loading, the more difficult dispersion becomes, especially for the starting ceramic powders with high specific surface area. Choice of solvent, dispersant, particle size and morphology of the powders will all affect the loading limit of the slurry, and consequently the drying behavior of the cast tape as well as the microstructure of the green tape<sup>3</sup>. Similarly, the choice of binder and plasticizer, and their loading levels, will affect the strength, durability and resistance to cracking of the green tape [4]. Finally, all of the above factors will influence the sintering shrinkage and final microstructure of the fired tape.

Glassy or eutectic forming additives is the general approach to reduce the sintering temperature of the ceramic. Recently

\* Corresponding author.

E-mail address: [jjbian@shu.edu.cn](mailto:jjbian@shu.edu.cn) (J.J. Bian).

**Table 1**

LTFO Glass-free slurry composition for tape casting.

Component	Function	Concentration (wt%)
Li <sub>2.08</sub> TiO <sub>3</sub> -LiF	Ceramic powder	50–60
Citrate acid (C <sub>6</sub> H <sub>8</sub> O <sub>7</sub> ·H <sub>2</sub> O)	Dispersant	0.3–1.2
Polyvinyl Butyral (PVB)	binder	6–10
Dibutyl phthalate (DBP)	Plasticizer	3–20
Polyethyleneglycol (PEG)	Plasticizer	
Ethanol	Solvent	30–40
Methyl ethylene ketone (MEK)	Solvent	

glass-free LTCC material with appropriate microwave dielectric properties is strongly desired for the multilayer structure applications because it simplifies the chemical interaction with the metal electrode and reduces the possibility of cracking caused by the mismatch of the coefficient of thermal expansion (CTE) between the ceramic and glassy phases [5,6]. A number of glass-free LTCC microwave dielectrics have been reported [7–14]. Although dozens of glass ceramic composite LTCC green tapes have been developed [15–21], only a few reports are available on the literature about the tape casting of glass free LTCC materials [22,23]. In our previous work we reported Li<sub>2.08</sub>TiO<sub>3</sub>-LiF glass-free LTCC material which could be densified at 900 °C/2 h and has good microwave dielectric properties:  $\epsilon_r \sim 22.8$ ,  $Q \times f \sim 63\,000$  GHz (~8 GHz) and  $\tau_f \sim 1.0$  ppm/°C [24]. The ceramic is also chemically compatible with Ag. In present paper we optimized different variables to prepare Li<sub>2.08</sub>TiO<sub>3</sub>-LiF glass-free LTCC green tape by tape casting process, and characterized the thermal and microwave dielectric properties of the sintered sheet. The sintering kinetics of the green tape and cofiring behavior with Ag electrode were also investigated.

## 2. Experimental

Li<sub>2.08</sub>TiO<sub>3</sub>-LiF (LTFO) ceramics were prepared by conventional solid-state reaction process from the starting materials including Li<sub>2</sub>CO<sub>3</sub> (99.9%), TiO<sub>2</sub> (99.7%) and LiF (99.9%). The starting materials were weighed according to the above formula and ball milled in ethanol with zirconia milling media for 24 h. Cylinder milling with 70 rpm was adopted. The slurry was then dried and calcined at 700 °C for 2 h in alumina crucible. The calcined powders were pulverized again by ball milling in ethanol for 24 h. The phase formation was confirmed by X-ray powder diffraction with Ni-filtered Cu Ka radiation (Rigaku D/max2200, Tokyo, Japan). The particle size distribution of the ground powder was determined by Dynamic Light Scattering (DLS) technique (Mastersizer-2000, Malvern, Worcestershire, UK). The BET surface area of the powder was measured from nitrogen adsorption isotherm using surface area analyzer (Nova-2000, Quantachrome, USA). The morphology of the particles was observed by transmission electron microscopy (TEM) (JEM-200CX, 100KV, JEOL, Japan).

Firstly dispersion studies were carried out with 8 wt% ceramic loading and varying dispersant amount from 0.3 to 1.5 wt%. The effectiveness of the dispersant was evaluated from the sedimentation of ceramic powders/dispersant/solvent system. A binary azeotropic mixture of ethanol (40 wt%) and methyl ethylene ketone (MEK, 60 wt%) was used as solvent. Citric acid was used as dispersant. The sedimentation analysis was carried out in a 10 ml graduated measuring cylinder. The initial height ( $H_0$ ) and sediment height ( $H$ ) at different time interval were noted. The first stage of slurry preparation is the dispersion of the ceramic powders in the solvent during which precalculated amount of ceramic powder was mixed with solvent and dispersant by ball milling for 8 h. The second stage involves mixing with the binder (polyvinyl butyral (PVB)) and plasticizer (Dibutyl phthalate (DBP)) and further ball milling for 24 h. The tape casting slurry composition in this study is given in Table 1. The viscosity and rheological property

were measured at room temperature using rheometer (RS6000, Thermo Fisher scientific, Germany). The final homogenized slurry was vacuum degassed and casted into thin tapes (~140 µm) using a tape-casting machine (LYJ-150, Dongfang Taiyang, Beijing, China). The casted tape was then allowed to dry at room temperature in ambient atmosphere for 24 h. Tensile strength of the green tape was measured using a Universal Testing Machine (Biaxial-10KN, ZWICK, Germany) at crosshead speed of 5 mm/min. The specimen gauge length was 40 mm, width 10 mm and thickness 0.11 mm. The debinding temperature of the green tape was determined by differential thermal analysis (DTA) and thermogravimetric analysis (TGA) (STA409C, NETZSCH, Germany). While sintering, the green tape was kept in between two thin Al<sub>2</sub>O<sub>3</sub> substrates in order to avoid warping and also to control the lateral ( $x, y$ ) shrinkage. The sintering shrinkage of the green tape at different heating rate was measured using heating microscope with automatic image analysis (EM201-15, Hesse Instruments, Germany). The microstructures of the green tape and sintered sheet (900 °C/2 h) were characterized by scanning electron microscopy (SEM) (Model JSM-6700F, JEOL, Tokyo, Japan). The sintered tape for SEM observation was polished and thermally etched at the temperature of 100 °C lower than its sintering temperature for 30 min. The density of the ceramic sheet was measured by the Archimedes method. The microwave dielectric properties of the ceramic sheet with thickness 0.11 mm were measured in a Split Post Dielectric Resonator operating at 20 GHz with the aid of a vector network analyzer (N5242A, Agilent, USA). The linear coefficient of thermal expansion (CTE) of the LTFO bulk ceramic sintered at 900 °C was measured using dilatometer (NETZSCH STA 449C, Netzsch Instrument, Germany) up to 300 °C. The thermal conductivity was measured using a laser flash thermal properties analyzer (LFA467, Netzsch Instrument, Germany). The break down strength of the ceramic sheet with thickness 0.11 mm was measured in silicon oil at room temperature with internal bias voltages up to 10,000 V by Ferroelectric analyzer (Model TF analyzer 2000E, aix ACCT system, Germany). Silver electrodes were coated on both polished surfaces of the sample and fired at 800 °C for 30 min to form a metal-insulator-metal capacitor for electrical test. In order to investigate the cofiring behavior of the green tape and Ag pastes, metallization pastes were screen printed layer by layer upon the green ceramic tape followed by stacking and lamination under the cold isostatic pressure of 40 MPa. The multilayer stack was sintered at 900 °C/2 h. The cross sectional surface of the sintered multilayer stack was polished and used to observe the interface microstructure and interdiffusion by back scattering SEM and corresponding EDS analysis.

## 3. Results and discussion

The powder XRD pattern of the LTFO calcined at 700/2 h shown in Fig. 1 demonstrates main phase with monoclinic rock salt structure with small amount of Li<sub>2</sub>CO<sub>3</sub>. The particle size distribution of the calcined powder after milling for 8 h is shown in Fig. 2a. It shows monomodal distribution. The average diameter is about 1.96 µm and BET specific surface area is about 6.24 m<sup>2</sup>/g, respectively. The TEM image of the calcined powders exhibits spherical particles (Fig. 2b), which is helpful to achieve high packing density.

Stabilization of ceramic suspension is critical for preparation of homogeneous tape casting slurry with good flowing properties. The stability of the suspension is usually evaluated from the sedimentation of ceramic powders/dispersant/solvent system. Fig. 3 shows the relative change of sediment height ( $\Delta H/H_0$ ) of the suspensions containing 8 wt% LTFO powders after keeping for 12 h as a function of citrate acid dispersant amount. The suspension containing 0.5 wt% citrate acid has the lowest rate of sedimentation. The stability of the suspension usually depends on the total

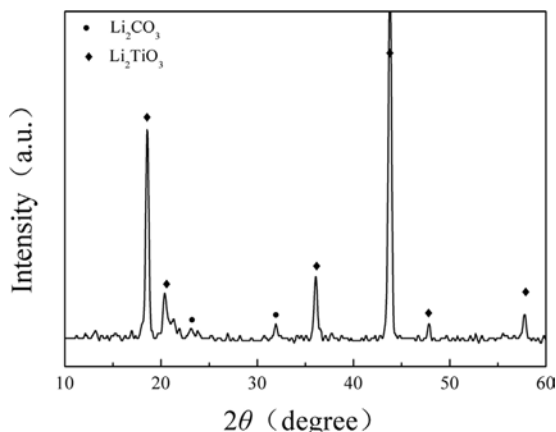


**Fig. 1.** XRD pattern of the LTFO powders calcined at 700 °C/2 h.

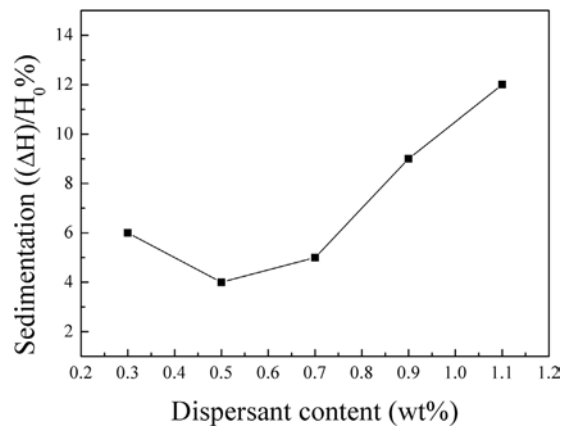


**Fig. 3.** Relative change of sediment height ( $\Delta H/H_0$ ) of the suspensions after keeping for 12 h as a function of citrate acid dispersant amount.

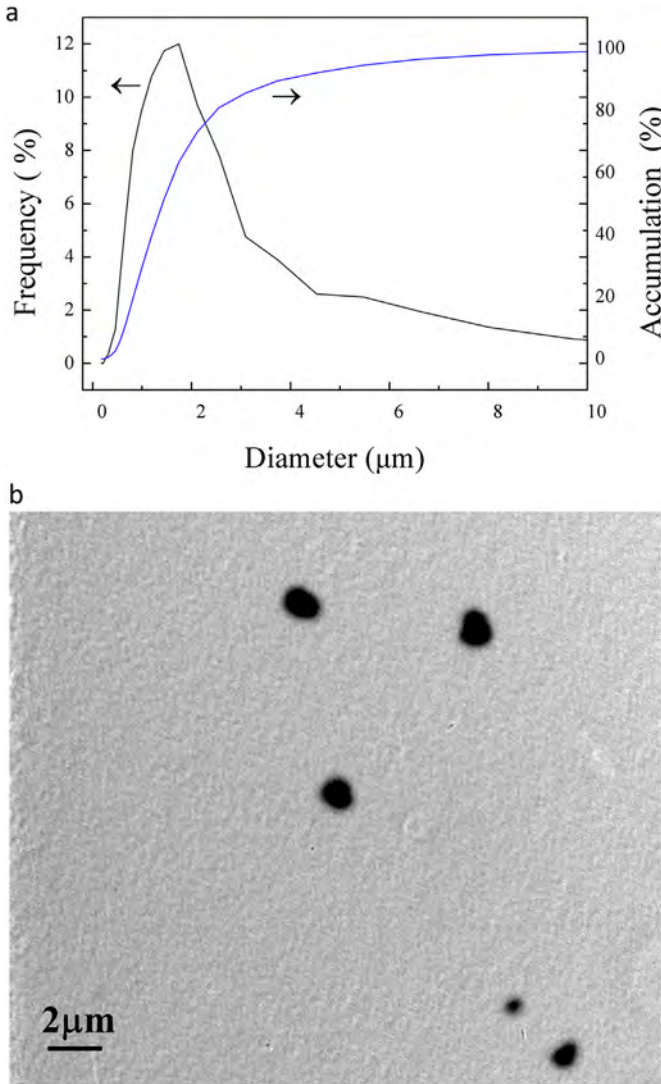


**Fig. 2.** (a) Particle size distribution and (b) TEM image of the calcined powders after milling for 8 h.

interparticle potential energy, mainly including attractive energy from long-range van der Waals interaction and repulsive potential energy from electrostatic and steric interactions between particles [25]. Since the effective steric stabilizing agent is usually macromolecular polymer [3]. So, in nonaqueous media like in this case,

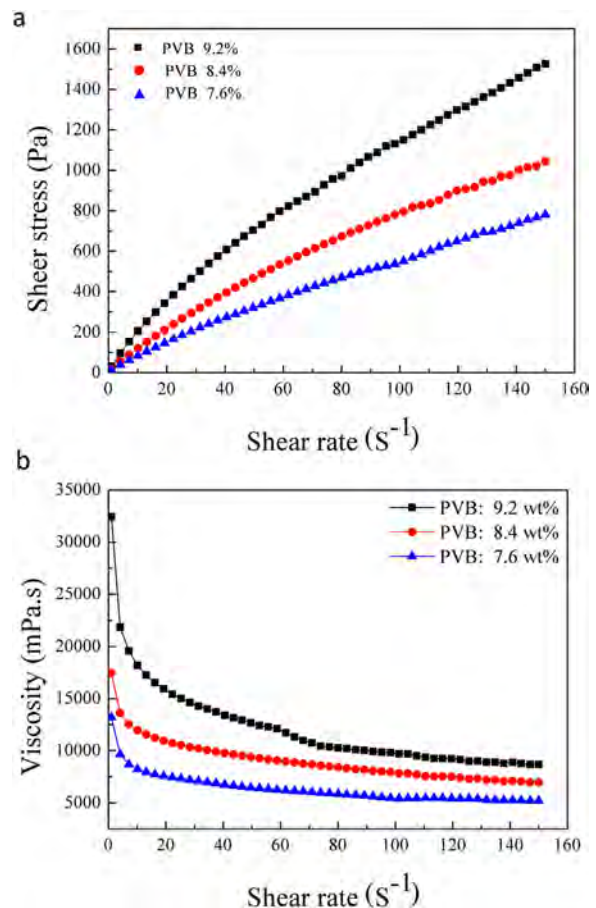


**Fig. 4.** (a) Flow curves (shear stress vs. shear rate) and (b) viscosity vs. shear rate for the slurries with different binder content.

the stabilization by citrate acid ( $\text{C}_6\text{H}_8\text{O}_7\text{-H}_2\text{O}$ ) dispersant should be dominated by electrostatic repulsion. The citrate acid adsorbed on the basic surface sites of the ceramic oxide particle was dissociated by transferring  $\text{H}^+$  to the surface site. Some dissociated anions desorbed into the solution leaving a positive charge on the particle surface. The powder loading depends on the density and particle size of the powder and the effectiveness of dispersant. The maximum powder loading attainable in this case is 54 wt%. Fig. 4 shows the rheological properties of the slurry with different binder content. Although the viscosity of the slurry increases with the increase

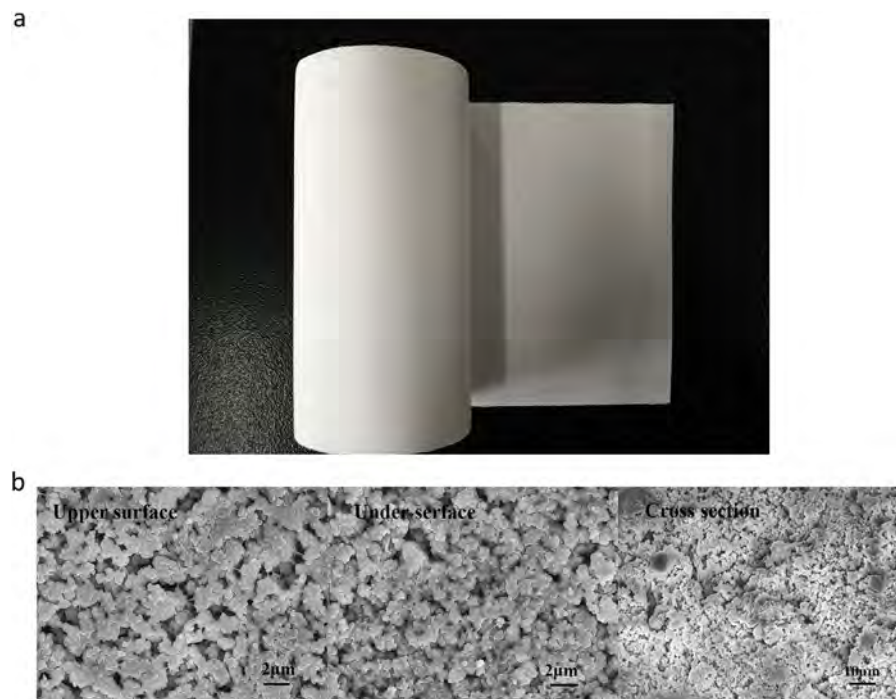


**Fig. 5.** (a) Photograph of the LTFO green tape and (b) SEM images of the green tape.

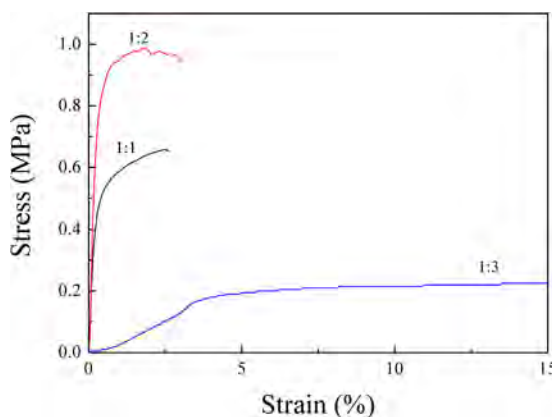


**Fig. 6.** Tensile strength of the LTFO green tape as function of ratio of binder/plasticizer. (For interpretation of the references to colour in this figure legend, the reader is referred to the web version of this article.).

in binder content as expected, all slurries demonstrate typical pseudoplastic (shear-thinning) behavior, which is essential to tape cast.

Fig. 5a shows the photograph of the LTFO green tape. The SEM images of the green tape shown in Fig. 5b demonstrate homogeneous microstructure. The relative density of the LTFO green tape is about 50% of theoretical density. The tensile strength of the LTFO green tape as function of ratio of binder/plasticizer is shown in Fig. 6. It indicates that the tensile strength decreases with the increase in plasticizer content as expected. The green tape with 1:3 ratio of binder/plasticizer exhibits plastic deformation as the stress exceeds 0.2 MPa. Maximum tensile strength of 0.9 MPa could be obtained when the ratio of binder/plasticizer is 1/2. Fig. 7 shows the DTA/TG analysis of the LTFO green tape. The burnout process of organic additives mainly occurred at 300 °C and completed at about 500 °C with total weight loss of ~30%. In order to study the sintering kinetics of the LTFO green tape, shrinkage curves of the green tape fired at different heating rates in air are shown in Fig. 8. As expected, the shrinkage curves shift to higher temperatures as the

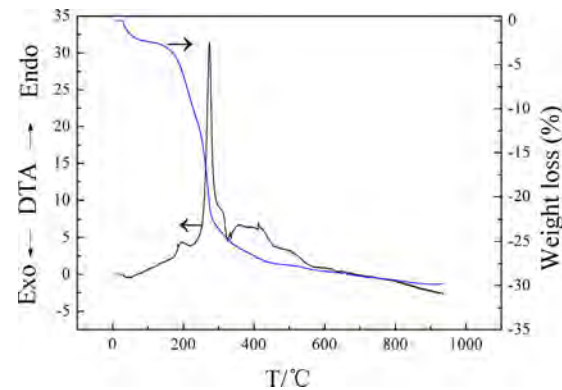


**Fig. 7.** DTA/TG analysis of the LTFO green tape. (For interpretation of the references to colour in this figure legend, the reader is referred to the web version of this article.)

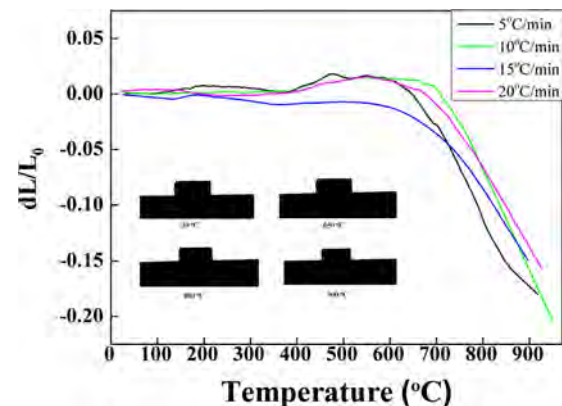


**Fig. 8.** Shrinkage curves of the green tape multilayer stack fired at different heating rates in air. (Inset shows the photographs of the multilayer stack fired at different temperatures). (For interpretation of the references to colour in this figure legend, the reader is referred to the web version of this article.)

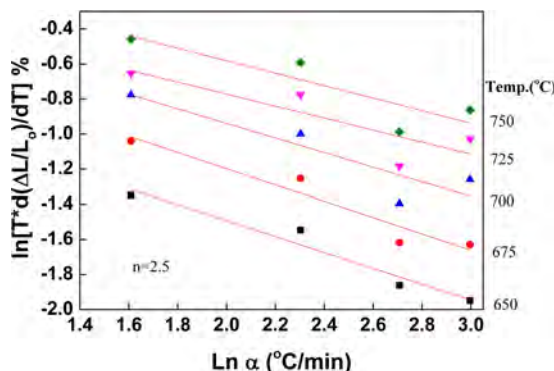


**Fig. 9.** Constant heating rate data in Fig. 8 reconstructed as  $\ln[Td(\Delta L/L_0)/dT]$  vs  $\ln(\alpha)$  at various firing temperatures.

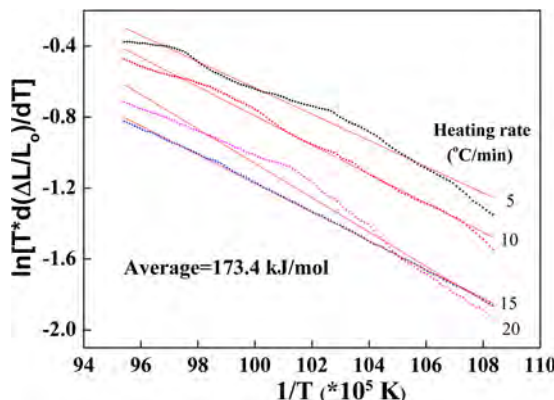
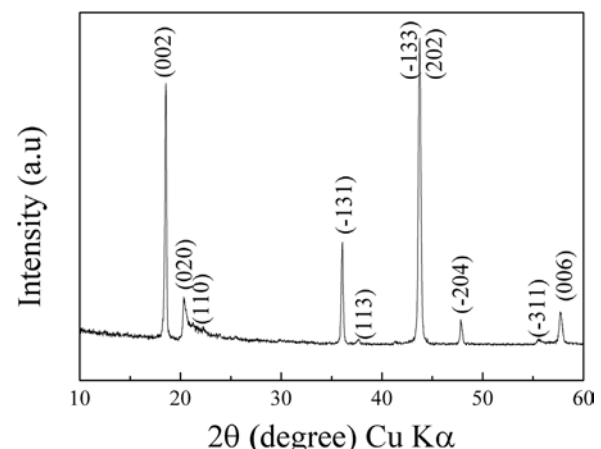


**Fig. 10.** Activation energies of the LTFO green tape determined at various heating rates. (For interpretation of the references to colour in this figure legend, the reader is referred to the web version of this article.)

heating rate is increased. The tape sintered at  $900^\circ\text{C}/2\text{ h}$  demonstrated shrinkage of 17% and 18.5% vertical and along the casting direction, respectively. The densification kinetics is determined on the basis of Kingery's analysis of liquid phase sintering using the following equation [26,27]:

$$\ln[Td(\Delta L/L_0)/dT] = \ln(\frac{1}{n}K_0^{\frac{1}{n}}) - \frac{1}{n}\ln a - \frac{E_a}{nRT} \quad (1)$$

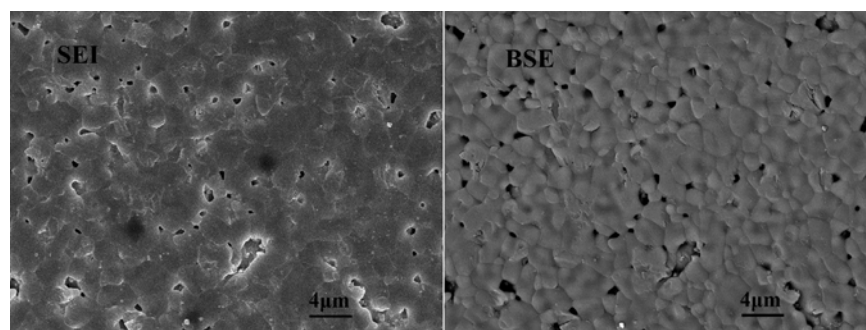
where  $\Delta L/L_0$  is the fractional shrinkage,  $T$  is the absolute temperature,  $n$  is the exponent,  $K_0$  is the preexponential term,  $\alpha$  is the heating rate,  $E_a$  is the apparent activation energy of sintering and  $R$  is gas constant. The detail procedure was described in reference [28]. Curves in Fig. 8 reconstructed as  $\ln[Td(\Delta L/L_0)/dT]$  vs  $\ln(\alpha)$  at various firing temperatures, as shown in Fig. 9. The slope of the straight line can be used to determine the values of  $n$  at different temperatures. The average value of  $n$  is about 2.5, which can be used



**Fig. 12.** XRD pattern of the LTFO tape sintered at  $900^\circ\text{C}/2\text{ h}$ .

to determine the apparent activation energy of the densification for LTFO green tape according to Eq. (1) by replotted data in Fig. 8 as  $\ln[Td(\Delta L/L_0)/dT]$  vs  $1/T$  at various heating rates, which is shown in Fig. 10. The average activation energy,  $E_a$ , is determined from the slopes of the straight lines to be  $\sim 173\text{ kJ/mol}$ . The low sintering activation energy can be ascribed to the presence of transient liquid phase from the melting of  $\text{Li}_2\text{CO}_3$  and defects during sintering process [24].

The microstructure of the sintered tape shown in Fig. 11 demonstrates well packed grains with fractional porosity. The relative density of the LTFO ceramic sheet is  $\sim 96\%$  TD after sintering at  $900^\circ\text{C}/2\text{ h}$ . The backscattering SEM images shows a monophasic microstructure, which is in well agreement with the XRD result shown in Fig. 12. The excessive  $\text{Li}_2\text{CO}_3$  phase remained in the calcined powders (Fig. 1) worked as transient reactive liquid phase sintering aid, decomposed at high temperature and precipitated into the matrix after sintering [24,29]. The microwave dielectric properties of the LTFO ceramic sheet are illustrated in Table 2. The microwave permittivity of the sheet is  $\sim 22.4$ , which is almost the same as that of the bulk sample (22.8), while the  $Q \times f$  value of the LTFO ceramic sheet is  $\sim 36,000\text{ GHz}$ , which is much lower than that obtained for the bulk counterpart (63,000 GHz). The BDS of the LTFO ceramic sheet measured at 50 Hz is 50 KV/mm and that obtained at DC bias condition is 120 KV/mm, which exhibits excellent insulating property (Table 2). Thermal properties including thermal expansion coefficient and thermal conductivity of the ceramic material are also important in LTCC technology, especially for the multichip module (MCM) applications. The thermal expansion coefficient (Fig. 13) and thermal conductivity obtained for the bulk LTFO ceramic is about 22.4 ppm/ $^\circ\text{C}$  and  $4.75\text{ W m}^{-1}\text{ K}$ , respectively. In order to investigate the cofiring behavior between the Ag paste and LTFO green tape, Fig. 14 shows the typical cross sec-

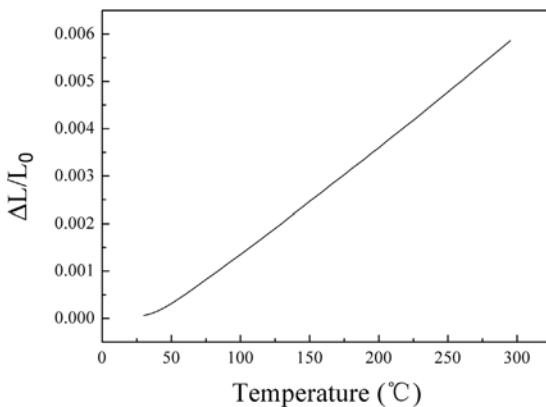


**Fig. 11.** SEM images of the tape sintered at  $900^\circ\text{C}/2\text{ h}$ .

**Table 2**

Microwave dielectric properties and BDS of the LTFO sintered tape.

Thickness	Measured frequency	$\epsilon_r$	$Q \times f$ GHz	BDS@50 Hz (kv/mm)	BDS@DC (kv/mm)
0.11 mm	20 GHz	22.4	35790 GHz	50	120

**Fig. 13.** Thermal expansion characteristics of the LTFO ceramic sintered at 900 °C/2 h.

tional SEM image and corresponding EDS analysis of the multilayer stack (8 layers) after isostatic pressure at 40 MPa and sintering at 900 °C/2 h. No warpage, crack and delamination could be observed. The corresponding EDS analysis demonstrates clear interface and no interdiffusion occurred between the layers of LTFO and Ag electrode. It indicates good chemical and sintering shrinkage compatibilities between the LTFO green tape and Ag thick film, which is crucial for practical LTCC fabrication.

#### 4. Conclusions

A glass-free low firing  $\text{Li}_{2.08}\text{TiO}_3\text{-LiF}$  ceramic has been prepared through the solid state ceramic route. The tape casting slurry of  $\text{Li}_{2.08}\text{TiO}_3\text{-LiF}$  with typical pseudoplastic behavior has been prepared and cast into thin tapes of thickness 110–140  $\mu\text{m}$ .  $\text{Li}_{2.08}\text{TiO}_3\text{-LiF}$  green tape shows a tensile strength of 0.9 MPa. The sintering activation energy of the green tape was determined to be  $\sim 173 \text{ kJ/mol}$ . The tape sintered at 900 °C/2 h demonstrated shrinkage of 17%–18.5% and relative density of 96.6% TD. The sintered single layer tape (110  $\mu\text{m}$ ) demonstrates good microwave dielectric properties:  $\epsilon_r = 22.4$  and  $Q \times f = 35490 \text{ GHz}$ . The ceramic sheet also demonstrates excellent insulating properties with BDS over 50 kV/mm. It has a coefficient of thermal expansion of 22.4 ppm/°C and thermal conductivity of  $4.75 \text{ W m}^{-1} \text{ K}^{-1}$ . The

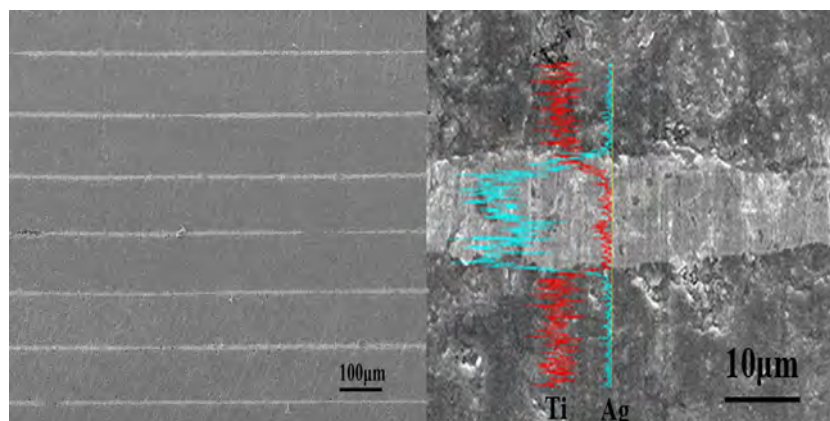
isostatic-laminated tape (8 layers) sintered at 900 °C/2 h shows good chemical and shrinkage compatibility during cofiring process.

#### Acknowledgements

The authors greatly appreciate Dr. Konig Jakob from Institute of Jozef Stefan, Slovenia, for his helping in the heating microscopy measurement.

#### References

- [1] Y. Imanaka, Multilayered Low Temperature Cofired Ceramics (LTCC) Technology, Springer, Boston, USA, 2005.
- [2] H. Jantunen, T. Kangasvieri, J. Vahakangas, S. Leppavuori, Design aspects of microwave components with LTCC technique, *J. Eur. Ceram. Soc.* 23 (2003) 2541–2543.
- [3] R. Moreno, The role of slip additives in the tape casting technology: part I-solvents and dispersants, *Am. Ceram. Bull.* 71 (10) (1992) 1522–1531.
- [4] R. Moreno, The role of slip additives in the tape casting technology: part II-Binder and plasticizers, *Am. Ceram. Bull.* 71 (10) (1992) 1647–1656.
- [5] M. Valant, D. Suvorov, Glass-free low-temperature cofired ceramics: calcium germanates, silicates and tellurates, *J. Eur. Ceram. Soc.* 24 (2004) 1715–1719.
- [6] J.J. Bain, D.W. Kim, K.S. Hong, Glass-free LTCC microwave dielectric ceramics, *Mater. Res. Bull.* 40 (21) (2005) 20–29.
- [7] G. Subodh, M.T. Sebastian, Glass-free  $\text{Zn}_2\text{Te}_3\text{O}_8$  microwave ceramic for LTCC applications, *J. Am. Ceram. Soc.* 90 (7) (2007) 2266–2268.
- [8] J.J. Bian, D.W. Kim, K.S. Hong, Microwave dielectric properties of  $\text{A}_2\text{P}_2\text{O}_7$  ( $\text{A} = \text{Ca}, \text{Sr}, \text{Ba}, \text{Zn}, \text{Mn}, \text{Mg}$ ), *Jpn. J. Appl. Phys.* 43 (6A) (2004) 3521–3555.
- [9] D.K. Kwon, M.T. Lanagan, T.R. Shroud, Microwave dielectric properties of  $\text{BaO}-\text{TeO}_2$  binary compounds, *Mater. Lett.* 61 (8–9) (2007) 1827–1831.
- [10] J.J. Bian, J.Y. Wu, L. Wang, Structural evolution, sintering behavior and microwave dielectric properties of  $(1-x)\text{Li}_3\text{NbO}_4-x\text{LiF}$  ( $0 \leq x \leq 0.9$ ), *J. Eur. Ceram. Soc.* 32 (2012) 1251–1259.
- [11] J. Li, L. Fang, H. Luo, J. Khalil, Y. Tang, C.C. Li,  $\text{Li}_4\text{WO}_5$ : a temperature stable low-firing microwave dielectric ceramic with rock salt structure, *J. Eur. Ceram. Soc.* 36 (1) (2016) 243–246.
- [12] D. Thomas, M.T. Sebastian, Temperature compensated  $\text{LiMgPO}_4$ : a new glass free low temperature cofired ceramic, *J. Am. Ceram. Soc.* 93 (2010) 3828–3831.
- [13] L. Sirdeshmukh, Y.R. Reddy, Dielectric properties of  $\text{Bi}_4(\text{GeO}_4)_3$  and  $\text{Bi}_4(\text{SiO}_4)_3$ , *Bull. Mater. Sci.* 2 (1980) 61–66.
- [14] Y.P. Liu, Y.N. Wang, Y.M. Li, J.J. Bian, Low temperature sintering and microwave dielectric properties of  $\text{LiMBO}_3$  ( $\text{M} = \text{Ca}, \text{Sr}$ ) ceramics, *Ceram. Int.* 24 (2016) 6475–6479.
- [15] T. Joseph, M.T. Sebastian, H. Jantunen, M. Jacob, H. Sreemoolanadhan, Tape casting and dielectric properties of  $\text{Sr}_2\text{ZnSi}_2\text{O}_7$  based ceramic-glass composite for low temperature co-fired ceramics applications, *Int. J. Appl. Ceram. Technol.* 8 (2011) 854–864.

**Fig. 14.** Typical cross sectional SEM image and corresponding EDS analysis of the multilayer stack (8 layers) after isostatic pressure at 40 MPa and sintering at 900 °C/2 h.

- [16] K. Manua, M.T. Sebastian, Tape casting of low permittivity Wesselsite–Glass composite for LTCC based microwave applications, *Ceram. Int.* 42 (2016) 1210–1216.
- [17] Y. Shimada, K. Utsumi, M. Suzuki, H. Takamizawa, M. Nitta, T. Watari, Low firing temperature multilayer glass-ceramic substrate, *IEEE Trans. CHMT-6* (4) (1983) 382–388.
- [18] T. Nishimura, S. Nakatani, S. Yuhaku, T. Ishida, Co-fireable copper multilayered ceramic substrate, *IMC 1986 Proceedings* (1986) 249–271.
- [19] H. Mandai, K. Sugoh, K. Tsukamoto, H. Tani, M. Murata, A low temperature co-fired multilayer ceramic substrate containing copper conductors, *IMC 1986 Proceedings* (1986) 61–64.
- [20] K. Niwa, N. Kamehara, K. Yokouchi, Y. Imanaka, Multilayer ceramic circuit board with a copper conductor, *Adv. Ceram. Mater.* 2 (4) (1987) 832–835.
- [21] S. Tosaka, S. Hirooka, N. Nishimura, K. Hoshi, N. Yamaoka, Properties of a low temperature fired multilayer ceramic substrate, *ISHM Proc.* (1984) 358.
- [22] P. Abhilash, M.T. Sebastian, K.P. Surendran, Glass free, non-aqueous LTCC tapes of  $\text{Bi}_4(\text{SiO}_4)_3$  with high solid loading, *Pullanchiyodan. J. Eur. Ceram. Soc.* 35 (2015) 2313–2320.
- [23] D. Thomas, P. Abhilash, M.T. Sebastian, Casting and characterization of  $\text{LiMgPO}_4$  glass free LTCC tape formicrowave applications, *J. Eur. Ceram. Soc.* 33 (2013) 87–93.
- [24] J.J. Bian, Y.M. Ding, A new glass-free LTCC microwave ceramic  $-(1-x)\text{Li}_2\text{TiO}_3 + x\text{LiF}$ , *Mater. Res. Bull.* 49 (2014) 245–249.
- [25] J.A. Lewis, Colloidal processing of ceramics, *J. Am. Ceram. Soc.* 83 (10) (2000) 2341–2359.
- [26] W.D. Kingery, Densification during sintering in the presence of liquid phase –I. Theory, *J. Appl. Phys.* 30 (3) (1959) 301–307.
- [27] J.H. Jean, T.K. Gupta, Isothermal and nonisothermal sintering kinetics of glass-filled ceramics, *J. Mtaer. Res.* 7 (12) (1992) 3342–3348.
- [28] J.H. Jean, C.R. Chang, Cofiring kinetics and mechanism of Ag-metallized ceramic-filled glass electronic package, *J. Am. Ceram. Soc.* 80 (12) (1997) 3084–3092.
- [29] J.J. Bian, Y.F. Dong, Sintering behavior, microstructure and microwave dielectric properties of  $\text{Li}_{2+x}\text{TiO}_3$  ( $0 \leq x \leq 0.2$ ), *Mater. Sci. Eng. B* 176 (2011) 147–151.